Journal of Micromechanics and Microengineering

PAPER

Interdigitated silver nanoelectrode arrays: a surface-enhanced Raman scattering platform for monitoring the reorientation of molecules under an external electric field

To cite this article: Y Yang *et al* 2019 *J. Micromech. Microeng.* **29** 124002

IOP Publishing Journal of Micromechanics and Microengineering
J. Micromech. Microeng. **29** (2019) 124002 (8pp) https://doi.org/10.1088/1361-6439/ab4b8e

Interdigitated silver nanoelectrode arrays: a surface-enhanced Raman scattering platform for monitoring the reorientation of molecules under an external electric field

Y Yang[1], **W J Sun**[1], **Y L Li**[1], **R H Pan**[1], **C Z Gu**[1,2] **and J J Li**[1,2,3]

[1] Beijing National Laboratory for Condensed Matter Physics, Institute of Physics, Chinese Academy of Sciences, PO Box 603, Beijing 100190, People's Republic of China
[2] School of Physical Sciences, University of Chinese Academy of Sciences, Beijing 100049, People's Republic of China
[3] Songshan Lake Materials Laboratory, Dongguan, Guangdong 523808, People's Republic of China

E-mail: jjli@iphy.ac.cn

Received 5 July 2019, revised 26 September 2019
Accepted for publication 7 October 2019
Published 23 October 2019

Abstract

In this paper, we propose a type of interdigitated silver nanoelectrode array fabricated by electron-beam lithography and ion beam etching. Ag nanoelectrode arrays with a width of 90 nm and a period of 150 nm have been successfully fabricated over a large area of 100 × 100 μm^2. The Ag interdigitated nanoelectrode arrays have been employed in surface-enhanced Raman scattering (SERS) measurements under different oscillating electric fields, in which the SERS signal of p-thiocresol (C_7H_8S) of 10^{-6} M was easily detected. Moreover, the intensity of the Raman modes exhibited distinguishable variations while changing the strengths and frequencies of electric field, which could be attributed to the field-induced stretching and distortion mechanics of molecular bonds. These results demonstrated that the Ag interdigitated nanoelectrode arrays would be a good candidate for sensing devices in the area of analytes detection, by taking advantage of the ability to modulate the orientation of molecules.

Keywords: interdigitated silver nanoelectrode arrays, SERS, electric field, p-thiocresol

(Some figures may appear in colour only in the online journal)

1. Introduction

Surface-enhanced Raman scattering (SERS) is an excellent technique for chemical and biological sensing due to its extremely high sensitivity, which has been demonstrated to be of the capability for single molecule detection [1–4]. SERS performance is mainly based on the excitation of localized surface plasmons, which are collective oscillations of conduction electrons on the surface of noble metal nanoparticles or nanostructures [5–9]. Based on the key technique used in fabrication processes, the fabrication methods for SERS substrates can be classified into two groups: chemical methods and physical methods [10]. Most of the chemical methods have been developed based on metal nanoparticles, whereas all the physical methods have employed planar nanofabrication techniques as the basic step.

In recent years, physical fabrication techniques such as ultraviolet lithography, electron beam lithography (EBL), and focused ion beam [11–15] have been widely employed in the fabrication of SERS substrate, due to notable advantages, including the high uniformity and reproducibility. Physical fabrication methods have been demonstrated to be a good choice to fabricate nanoelectrodes, promising applications in electronic devices and molecular devices [16–19]. Plasmonic nanoelectrodes, which combine both the electrical measurement and SERS capability, have become more and more attractive in recent years because of their potential applications in biological sensing devices [20–22]. However, in previous

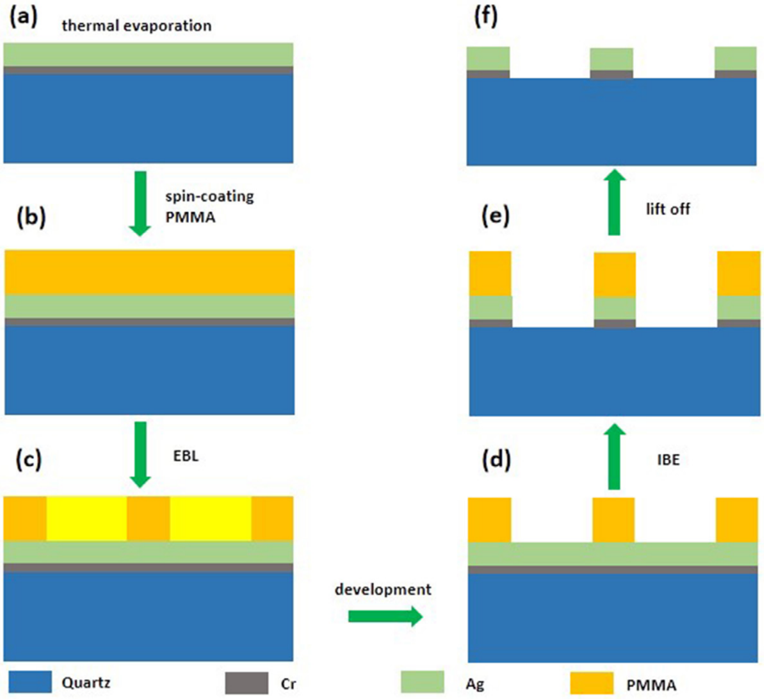

Figure 1. Schematic fabrication procedures of the Ag interdigitated nanoelectrode arrays on a quartz substrate.

reports, most of the SERS substrates are used to examine one type of molecule. In some cases of practical application of SERS, the analyte is in a mixture of different molecules, of which the spectral features are similar. It is still a challenge to discretely detect target molecules in a mixture with multiple analytes, although SERS has been demonstrated to be a powerful tool to detect molecules with ultra-low concentration.

It has been demonstrated recently that the SERS signal of molecules exhibited distinct variations under an external electric field, which are useful for studying molecule adsorption on charged surfaces and direct detection of the molecule in a mixture with multiple analytes. Sriram *et al* employed an electric field on silver nanotextured electrode pairs, and observed the changes in the SERS signal of thiophenol that originates from the electric field induced bending and stretching of the atomic band [23]. Further, thiophenol in a mixture of two analytes (thiophenol and benzyl mercaptan) has successfully been identified by applying an external electric field [24]. In addition to planar electrodes, tip-enhanced Raman spectroscopy (TERS) has been widely employed in electrochemistry (EC), which is of interest in investigating nanoscale EC with optical spectroscopy [25]. Sabanés *et al* used so-called EC-TERS to observe the electric field induced deprotonation and reorientation of the adenine molecule [26].

In most previous reports it has been found that the gap between electrodes is smaller than 10 nm in order to fit the size of small molecules. However, fabricating sub-10 nm nanoelectrodes over a large area is still challenging due to the critical technical procedures. In contrast, the fabrication techniques of nanogaps with tens of nanometre width are relatively mature, and are feasible to realize a large area. Therefore, a type of large-gap-size nanoelectrode that has the capability of both electrical tuning and SERS activity is attractive from the viewpoints of both fabrication and application. In recent years, interdigitated nanoelectrodes have attracted more and more attention due to their application in biological sensing devices and the feasibility in nanofabrication processes [27–29]. However, the influence of electric field on the small molecules absorbed on interdigitated nanoelectrodes is limited, although this is very important in terms of biological and environmental analysis. Further studies are needed in order to fully understand the influence of an electric field on the SERS spectra.

In this work, uniform Ag interdigitated nanoelectrode arrays have been successfully fabricated over a large area of $100 \times 100\ \mu\text{m}^2$ using EBL and ion beam etching (IBE), and were used as a SERS substrate in order to study the influence of external electric fields on the SERS spectra of a C_7H_8S molecule. Remarkably, the intensity of the Raman modes exhibited distinct fluctuations while changing the strength and frequencies of an oscillating electric field. These phenomena could be attributed to the field-induced reorientation of molecules. Our results suggest that the Ag interdigitated nanoelectrode arrays would be a good candidate for a sensing device in the application of analyte identification.

2. Experimental details

2.1. Ag interdigitated nanoelectrode array fabrication

The fabrication of interdigitated nanoelectrode arrays mainly includes six steps, as shown in figure 1. First, 5 nm Cr film and 50 nm Ag film were deposited onto a quartz substrate (thickness of 500 μm) that has been ultrasonically cleaned in acetone, alcohol and deionized water sequentially, as shown in figure 1(a). Second, poly(methyl methacrylate) (PMMA) (495 k, 5%) electron resist was spin-coated on the substrate, and was pre-baked

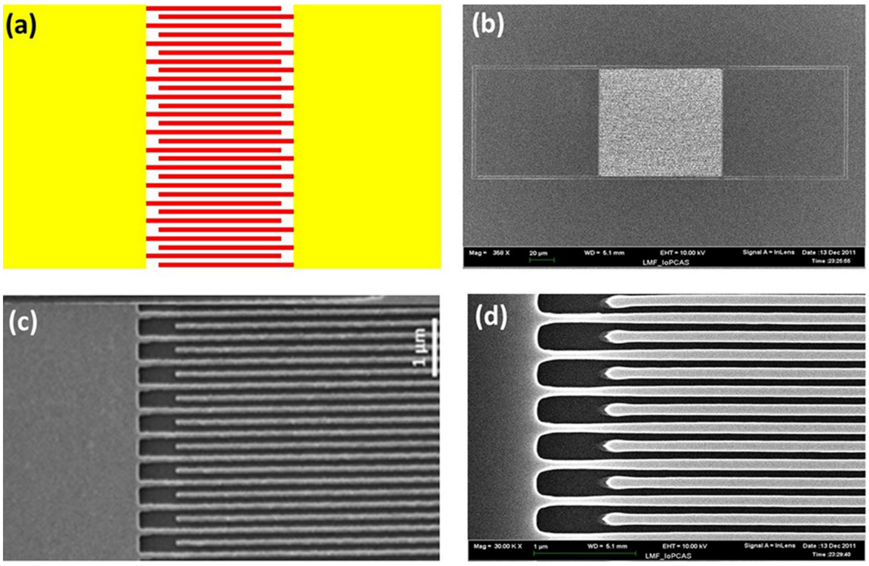

Figure 2. (a) A schematic image and (b)–(d) SEM images of interdigitated silver nanoelectrode arrays.

on a hot plate at 180 °C for 60 s, as shown in figure 1(b). Third, the sample was exposed by an EBL system (Raith 150) at 20 kV, as presented in figure 1(c). After that, the exposed sample was developed in a methyl isobutyl ketone (MIBK): isopropanol (IPA) (1:3) developer at room temperature, for 40 s, and then rinsed in IPA for 30 s and blown dry by pure nitrogen gas. As a result, the nano-patterns were formed in the electron resist layer, as shown in figure 1(d). Fifth, the nano-patterns of the electron resist layer were transferred to Ag film by IBE, as shown in figure 1(e). The top-down approach of IBE can avoid a large area lift-off process, and it has a high selection ratio of the photoresist mask to silver film, which is very suitable for precise fabrication of interdigitated nanoelectrodes. Finally, silver interdigitated nanoelectrode arrays were obtained after removing the PMMA resist using acetone, as shown in figure 1(f).

Figure 2 shows the scanning electron microscope (SEM) images of the Ag interdigitated nanoelectrode arrays fabricated following the procedures in figure 1. As exhibited in figure 2(b), the nanoelectrode arrays over a large area 100 × 100 μm^2 have been successfully fabricated. The width of the silver lines is about 90 nm and the period is about 150 nm. One can see clearly in figure 2(c) that the adjacent nanoelectrodes are well isolated from each other.

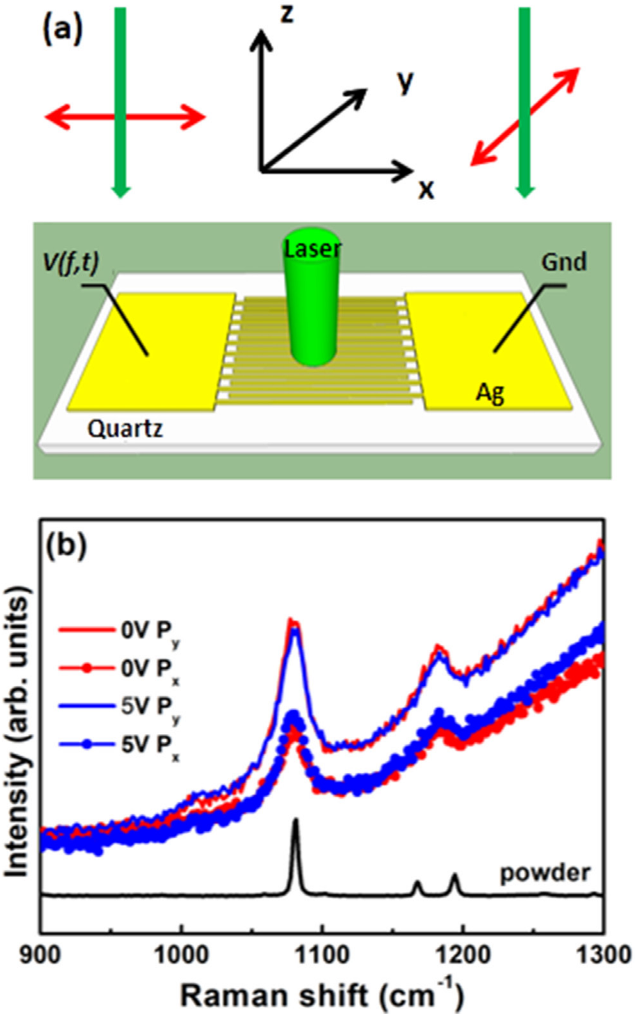

Figure 3. (a) Schematic of the SERS experiment measurement. (b) Typical SERS spectra of C_7H_8S with different polarization directions of the incident laser, collected with and without electric field. The Raman spectrum of C_7H_8S powder is inserted for reference.

2.2. SERS measurements

Before the SERS measurements, the sample was immersed in a C_7H_8S ethanol solution (10^{-6} M) for two hours, and then washed with ethanol for 10 min to guarantee that there was only one monolayer of C_7H_8S molecules adsorbed on the sample surface. Then, the SERS spectra were detected using a confocal Raman spectrometer (Renishaw inVia). The wavelength of the excitation laser used for SERS measurements was 514 nm and the laser power on the sample was about 0.9 mW. The spectra acquisition time is 60 s and a 50× long working distance objective lens was used for focusing the laser on the sample surface. As illustrated in figure 3(a), the

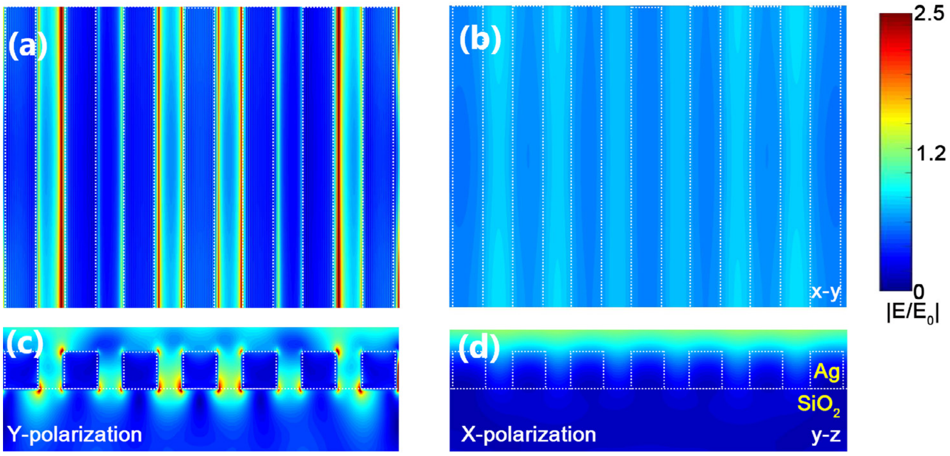

Figure 4. (a) and (b) Top view and (c) and (d) cross-sectional view of the calculated electric field distribution on Ag interdigitated electrodes without external electric field.

laser beam was normal incident onto the sample surface, and the polarization direction of the incident laser was along the x-axis and y-axis, respectively. In another words, the SERS signal were collected while the incident polarization was parallel and perpendicular to the direction of nanoelectrodes, respectively. The external electric field was supplied using a signal generator (Stanford Research System (SRS) model DS345, 30 MHz synthesized function generator).

2.3. Simulation methods

The finite-different time-domain (FDTD) method was employed to simulate the electric field distribution on the Ag interdigitated nanoelectrode arrays. The wavelength of the incidence light was set at 514 nm and propagated along the z-axis with the electric field polarized along the x- and y-axis, respectively. All the simulated boundaries were perfectly matched layers to avoid reflections. Two monitors were placed perpendicular to the x- and z-axis, respectively, to capture the field distribution.

3. Results and discussion

Figure 3(b) presents the typical SERS spectra of C_7H_8S under the different polarization directions of the laser, collected with and without external electric fields. Two peaks at 1080 cm^{-1} and 1190 cm^{-1} can be clearly seen, indicating the SERS ability of the fabricated Ag interdigitated nanoelectrode arrays. But these peaks are a little broadening, and fewer peaks can be detected compared with the Raman spectrum from C_7H_8S powder. This can be attributed to the increased background due to interaction between the molecule and Ag nanoelectrodes. One can see that the intensity of the Raman peaks under y-polarization excitation is obviously stronger than that under x-polarization excitation, regardless of measuring with or without an external electric field. This result comes from the inherent optical properties of Ag nanoelectrode arrays. According to the electromagnetic theories of SERS, the enhanced electromagnetic field of the incident laser is due to the localized surface plasmons resonance (LSPR), in which the electrons coherently oscillate locally within and in the vicinity of a nanostructure, particularly on the edges and tips of nanostructure or across nanogaps with sub-10 nm width [11, 30, 31].

In order to clarify the mechanism of SERS enhancement on the Ag interdigitated electrode arrays, the FDTD simulation was continued to evaluate the electromagnetic field distribution of the Ag nanoelectrodes arrays under different incident polarization. Figure 4 shows the map of simulated electric field enhancement $|E/E_0|$ on the surface of the nanoelectrodes. E is the local electric field at the surface and E_0 is the incident electric field. It is noteworthy that the maximum value of the enhanced field under y-polarization (figure 4(a)) is much higher than that obtained under x-polarization (figure 4(b)). These simulated results are consistent with the experimental results. What is more, one can see that the maximum amplitude of the electric field is localized on the surface of the Ag electrodes, whatever the polarization of the incident laser is along the x-axis or y-axis, although the grade of field enhancement is hugely different. As illustrated in figure 4(c), the highest electric field appears on the edge of electrodes, whereas the field strength is much lower in the gap between two adjacent electrodes. The size of the gap is 60 nm in our work, which is much larger than the correlation length of LSPR, so that the highest electric field takes place on the edges of electrodes. This is consistent with a previous publication, in which Yue *et al* reported that the hot spots were located at the edge of the gold split ring resonators rather than in the gaps with width larger than 50 nm [31].

Comparing the results exhibited in figures 4(a) and (b), the electromagnet field enhancement at y-polarization is nearly four times that at x-polarization. As the Raman enhancement is proportional to the biquadratic of electric field enhancement ($|E/E_0|^4$), the peak intensity of the Raman modes at y-polarization should be over 200 times higher than at x-polarization. However, as presented in figure 3(b), the measured the Raman intensity at y-polarization is just two times that obtained at x-polarization. This discrepancy can be attributed to the very small areas of the hot spots in a laser spot with a diameter of ~2 μm. Apart from the edges, the field enhancement on the other parts of the nanoelectrodes are very close between the *y*-polarization and *x*-polarization excitations. As a result, the average field enhancement in a laser spot under *y*-polarization is just several times higher than that under *x*-polarization.

As presented in figure 3(b), the SERS spectra do not exhibit obvious changes under a certain electric field. In order to gain a deeper insight into the influence of the external electric field on the SERS response, SERS spectra were measured under different field strengths (5 mv, 20 mv, 50 mv, 100 mv) and frequencies (1 mHz, 100 mHz, 1 Hz, 10 Hz, 100 Hz, 1 kHz, 10 kHz). Figure 5 presents the typical spectra collected at different strengths and frequencies of the electric field, in which the intensity of Raman peaks exhibited obvious changes, particularly the peak located at around 1080 cm^{-1}, while changing the external electric field.

Figure 5(a) shows the SERS spectra collected at different field strengths with a fixed frequency of 1 Hz. One can see clearly in figure 5(a) that the intensity of Raman peaks fluctuates with increasing field strengths. The peak intensity starts to decrease with increasing electric potential, and reaches the lowest value at 20 mV. The peak intensity at 20 mV is only half of that at 0 mV. Then, the intensity increases a little with a higher electric field, and the intensity at 100 mV recovers to 65% of that at 0 mV. Figure 5(b) shows the SERS spectra collected at different electric frequencies with a fixed field strength of 20 mV. It noteworthy that the intensity drops to the lowest value at 1 Hz, about half of that at 0 Hz. Then, the intensity increases with increasing frequency, reaches 76% of that at 0 Hz.

In order to systematically investigate the correlation between SERS intensity and electric field, the SERS spectra collected at different electric fields were deconvoluted into components using a Lorentz/Gaussian mixed function, and the peak intensities were normalized using the SERS results collected regularly at zero field. This allowed for the absolute intensities of individual components in the SERS spectra at different field strengths to be obtained. Figure 6 presents the dependences of the SERS intensity of the 1080 cm^{-1} peak as a function of field strengths and frequencies, in which several remarkable phenomena can be observed clearly. First, the peak intensity exhibits obvious changes with variable frequencies. Furthermore, the variation traces of the peak intensity at different electric field strengths are different from each other. Second, one can see that the intensities at *x*-polarization and *y*-polarization exhibit distinct variations with increasing frequencies. At a certain frequency, the intensity at *y*-polarization significantly increases, whereas the intensity at *x*-polarization decreases. Third, the position of the highest/lowest intensity shifts to lower frequency with increasing field strengths. Last but not least, the biggest discrepancy of intensity between *x*- and *y*-polarization occurs at 20 mV. It is worth noting that the intensity at *y*-polarization is around ten times that at *x*-polarization. In contract, the intensity ratio between *y*-polarization and *x*-polarization is just 2.8 at 100 mV.

As shown in figure 6, applying an external electric field on the Ag interdigitated nanoelectrode arrays causes the enhancement or suppression of the SERS signal. The variation traces of intensity are complicated with different field strengths and frequencies. Consequently, the SERS intensity of the 1080 cm^{-1} peak via field strength and frequency was created as a 2D image, and presented in figure 7. One can see that the SERS intensity varies significantly while changing the electric potential and frequencies, suggesting the strong SERS intensity dependence on the external electric field. In addition, the maximum intensity at *x*-polarization occurs at 80 mV with 100 mHz (figure 7(a)), whereas the maximum intensity at *y*-polarization occurs at 20 mV with 1 Hz (figure 7(b)). These results are in good agreement with those presented in figure 6.

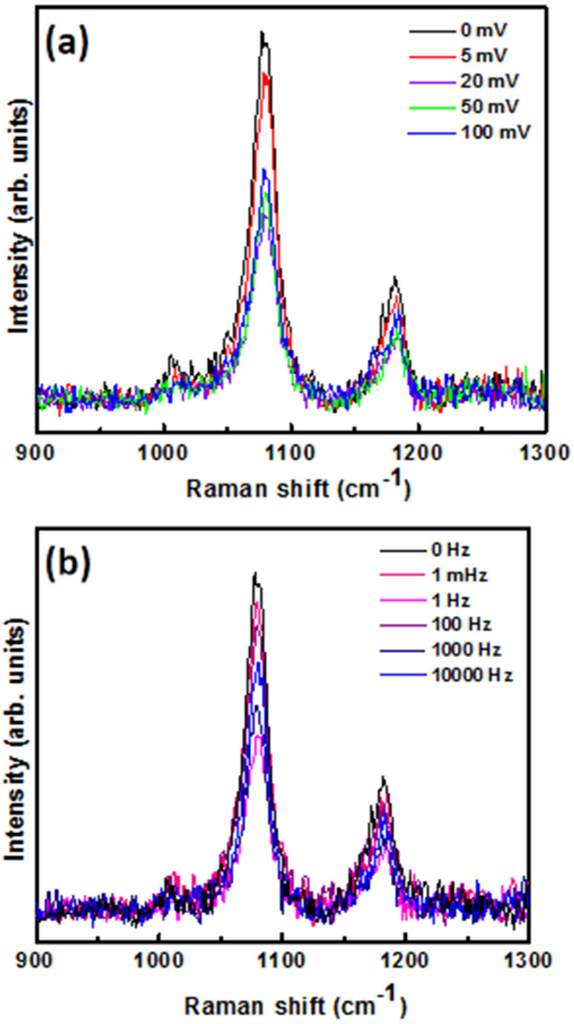

Figure 5. SERS spectra collected at different (a) field strengths and (b) frequencies.

As presented in figures 5–7, the SERS intensity of the C_7H_8S molecules exhibited remarkable dependence on the external electric field, demonstrating that both the field strength and frequency could affect the SERS intensity. The field strength effect on the SERS intensity can be attributed to the molecule realignment with respect to the direction of the electric field. It is well known that two major mechanisms, including physical and chemical mechanisms, are accepted for extreme SERS enhancement. The physical mechanism is also called the electromagnetic field enhancement mechanism, in which the electromagnetic field of both the incident and scattered light are extensively enhanced due to the LSPR on the

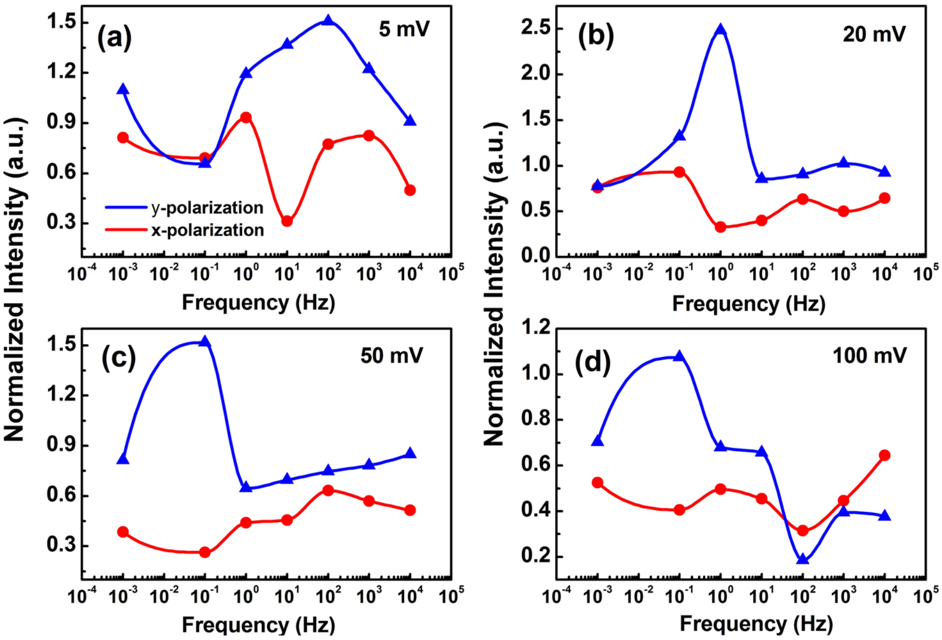

Figure 6. The trends in relative peak intensity for the 1080 cm^{-1} peak at different frequencies, normalized to the case of no electric field, are shown for electric fields: (a) 5 mV, (b) 20 mV, (c) 50 mV and (d) 100 mV.

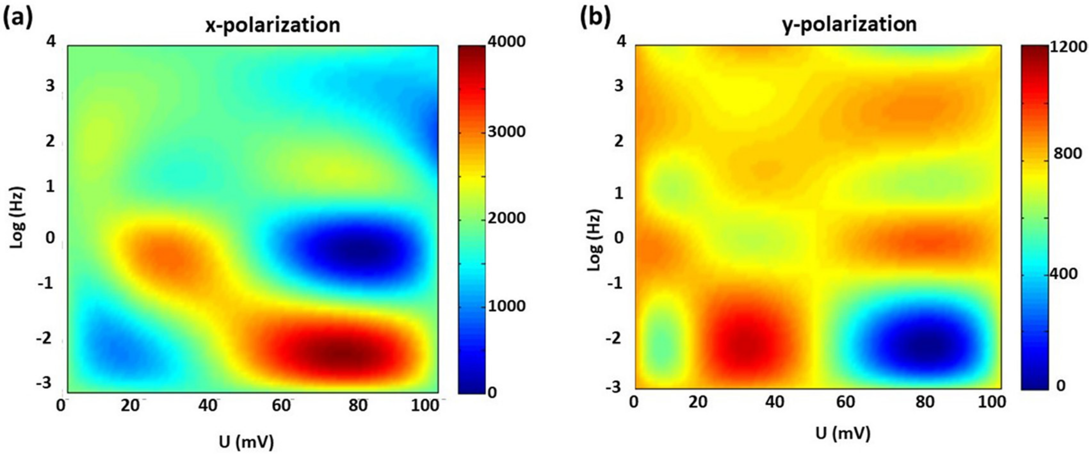

Figure 7. 2D images of SERS intensity via electric potential and frequency at (a) *x*- and (b) *y*-polarization.

metal nanostructures. This contribution has been discussed in figure 4, which is mainly related to the geometry of nanostructures. The chemical mechanism is the so-called charge transfer (CT) enhancement mechanism, in which electrons exchange between the molecule and the metal surface through the covalent bond under a light-exited electron transition [32, 33]. Applying an external electric field, new CT transition states are produced by the interaction between the metal and adsorbed molecule proposed by density functional theory (DFT) and time-dependent density functional theory simulations (TD-DFT) [34]. Recently, Zhang *et al* have demonstrated a field-induced transition from the traditional excited state to a pure CT excited state, and that the CT transition produces enhanced Raman intensities [35]. The chemical enhancement mechanism contributes to the increase of polarizability [36]. C_7H_8S is a polar molecule consisting of a benzene ring with a methyl and a thiol, which is binding to the surface of Ag interdigitated nanoelectrodes through the S atom by cleavage of the S–H bond. The C_7H_8S molecules are supposed to vertically absorb on the nanoelectrodes with specific angles to the normal direction of the nanoelectrodes surface. Applying an electric field slightly changes the equilibrium geometry and polarizabilities of the C_7H_8S molecules. The corresponding vibrational modes can be decomposed with certain vibration vectors along the direction of the applied fields, leading to the specific Raman enhancement. As a result, the external electric field selectively enhances some Raman modes through changing its magnitude and orientation.

In addition to the dependence on field strength, it is striking that the intensity fluctuates under different field frequencies. Under an oscillating electric field, the molecule bonds are forced to constantly realign, and their net polarization adjusts the direction with respect to the direction (polarity) of the electric field [23]. While alternating the external electric field, the

S–Ag bond compresses or stretches, leading to the stretching or distortion of the benzene ring, which tilts closer or away from the metal surface. As reported in previous publications, the 1080 cm^{-1} peak originates from the C–C stretching on the benzene ring [23, 24]. Therefore, the observed remarkable oscillation of the 1080 cm^{-1} peak in our work reveals the stretching or distortion in the benzene ring, while changing the frequency of electric field. Although the molecular orientation has been modulated by the external field, the orientation of the benzene ring can be realigned by a high oscillating frequency at a lower electric field, as shown in figures 6(a) and (b). As the acquisition time was 60 s in our work, it means that the fields with frequencies lower than 17 mHz could be considered quasi-static, whereas the number of electric field oscillations are averaged for frequencies exceeding 17 mHz. At a higher amplitude of electric field, the orientation of the benzene ring has been fixed, so that it needs a longer time to realign. As presented in figures 6(c) and (d), the maximum SERS intensity appears at relative low frequencies for higher field strength. Therefore, a proper field strength and frequency can cause the resonance of a specific vibrational mode of C_7H_8S through field-induced molecular reorientation. This demonstrates that the Ag interdigitated nanoelectrode arrays fabricated in our work are sensitive to the C–C vibration in the benzene ring, suggesting its application in the identification of molecules with a benzene ring.

As can be seen in this report, the SERS sensitivity of the current Ag interdigitated nanoelectrode arrays is at 10^{-6} M, which may hinder its application in single molecule detection. As we know, several kinds of high sensitivity SERS platforms have been developed based on chemical methods [10]. Recently, a so-called slippery liquid-infused porous surface-enhanced Raman scattering method was proposed, which has reached a detection limit down to the aM level [37]. Therefore, combining interdigitated nanoelectrode arrays with other SERS platforms would be the pathway for further development of interdigitated nanoelectrode arrays.

4. Conclusion

In this work, Ag interdigitated nanoelectrode arrays have been successfully fabricated over a large area using EBL and IBE. The Ag nanoelectrode arrays were employed as a SERS substrate and used to study the external electric field effect on the SERS response of C_7H_8S molecule. It is worth noting that the intensity of the specific vibrational mode of the C_7H_8S exhibited remarkable variations under different field strengths and frequencies, which could be attributed to the changes in the polarizability of molecules due to the field-induced reorientation of molecules. Our results demonstrate that Ag interdigitated nanoelectrode arrays would be a good candidate for sensing devices in the application of distinguishing molecule species through dynamic tuning SERS spectra, by employing an external electric field.

Acknowledgments

The authors acknowledge the financial support received from the National Key R&D Program of China (Grant No. 2018YFB0703500, 2016YFA0200800, and 2016YFA0200400), the National Natural Science Foundation of China (Grant No. 11704401, 11674387, 91323304, and 61390503), the Key Research Program of Frontier Sciences of Chinese Academy of Sciences (Grant No. QYZDJ-SSW-SLH042), and the Scientific Equipment Development Project of Chinese Academy of Sciences (Grant No. YJKYYQ20170027).

ORCID iDs

Y Yang https://orcid.org/0000-0003-3785-9233
Y L Li https://orcid.org/0000-0001-8266-0085
C Z Gu https://orcid.org/0000-0002-2689-2807
J J Li https://orcid.org/0000-0002-1508-9891

References

[1] Blackie E J, Le Ru E C and Etchegoin P G 2009 *J. Am. Chem. Soc.* **131** 14466
[2] Lacharmoise P D, Le Ru E C and Etchegoin P G 2009 *ACS Nano* **3** 66
[3] Nie S and Emory S R 1997 *Science* **275** 1102
[4] Li J F *et al* 2010 *Nature* **464** 392
[5] Shafer-Peltier K E, Haynes C L, Glucksberg M R and Van Duyne R P 2003 *J. Am. Chem. Soc.* **125** 588
[6] Xu S, Ji X, Xu W, Zhao B, Duo X, Bai Y and Ozaki Y 2005 *J. Biomed. Opt.* **10** 031112
[7] Douglas P, Stokes R J, Graham D and Smith W E 2008 *Analyst* **133** 791
[8] Qian X, Peng X H, Ansari D, Yin-Goen Q, Chen G Z, Shin D M, Yang L, Young A N, Wang M D and Nie S 2008 *Nat. Biotechnol.* **26** 83
[9] Stokes R J, McBride E, Wilson G C, Girkin J M, Smith W E and Graham D 2008 *Appl. Spectrosc.* **62** 371
[10] Yang Y, Gu C Z and Li J J 2019 *Small* **15** 1804177
[11] Pan R H *et al* 2018 *Nanoscale* **10** 3171
[12] Duan H, Hu H, Kumar K, Shen Z and Yang J K W 2011 *ACS Nano* **5** 7593
[13] Koh A L, Fernández-Domínguez A I, McComb D W, Maier S A and Yang J K W 2011 *Nano Lett.* **11** 1323
[14] Cui A, Liu Z, Dong H, Wang Y, Zhen Y, Li W X, Li J J, Gu C Z and Hu W P 2015 *Adv. Mater.* **27** 3002
[15] Kim M-K, Sim H, Yoon S J, Gong S-H, Ahn C W, Cho Y-H and Lee Y-H 2015 *Nano Lett.* **15** 4102
[16] Barik A, Chen X and Oh S-H 2016 *Nano Lett.* **16** 6317
[17] Yoo D, Gurunatha K L, Choi H K, Mohr D A, Ertsgaard C T, Gordon R and Oh S-H 2018 *Nano Lett.* **18** 3637
[18] Song H, Reed M A and Lee T 2011 *Adv. Mater.* **23** 1583
[19] Li T, Hu W P and Zhu D B 2010 *Adv. Mater.* **22** 286
[20] Tsutsui M, Taniguchi M, Yokota K and Kawai T 2010 *Nat. Nanotechnol.* **5** 286
[21] Ohshiro T, Matsubara K, Tsutsui M, Furuhashi M, Taniguchi M and Kawai T 2012 *Sci. Rep.* **2** 501
[22] Lesser-Rojas L, Ebbinghaus P, Vasan G, Chu M-L, Erbe A and Chou C F 2014 *Nano Lett.* **14** 2242

[23] Sriram S, Bhaskaran M, Chen S, Jayawardhana S, Stoddart P R, Liu J Z, Medhekar N V, Kalantar-Zadeh K and Mitchell A 2012 *J. Am. Chem. Soc.* **134** 4646
[24] Walia S, Shah A K, Stoddart P R, Bhaskarana M and Sriram S 2015 *Phys. Chem. Chem. Phys.* **17** 7095
[25] Zaleski S, Wilson A J, Mattei M, Chen X, Goubert G, Cardinal M F, Willets K A and Duyne R P V 2016 *Acc. Chem. Res.* **49** 2023
[26] Sabanés N M, Ohto T, Andrienko D, Nagata Y and Domke K F 2017 *Angew. Chem., Int. Ed.* **56** 9796
[27] Alayo N, Fernández-Sánchez C, Baldi A, Esquivel J P, Borrisé X and Pérez-Murano F 2016 *Microchim. Acta* **183** 1633
[28] Bonanni A, Fernández-Cuesta I, Borrisé X, Pérez-Murano F, Alegret S and Valle M 2010 *Microchim. Acta* **170** 275
[29] Li Z, Yu Y, Li Z, Wu T and Yin J 2015 *Anal. Methods* **7** 9732
[30] Ding S Y, You E M, Tian Z Q and Moskovits M 2017 *Chem. Soc. Rev.* **46** 4042
[31] Yue W, Yang Y, Wang Z, Chen L and Wang X 2013 *J. Phys. Chem.* C **117** 21908
[32] Jensen L, Aikens C M and Schatz G C 2008 *Chem. Soc. Rev.* **37** 1061
[33] Yamamoto Y S and Itoh T 2016 *J. Raman Spectrosc.* **47** 78
[34] Zhao X and Chen M 2014 *J. Raman Spectrosc.* **45** 62
[35] Zhang Y, Shao Y, Zhang W, Feng Y and Lin W 2016 *J. Raman Spectrosc.* **47** 310
[36] Arenas J F, Fernandez D J, Soto J, Lopez-Tocon I and Otero J C 2003 *J. Phys. Chem.* B **107** 13143
[37] Yang S, Dai X, Stogin B B and Wong T-S 2016 *Proc Natl Acad. Sci.* **113** 268